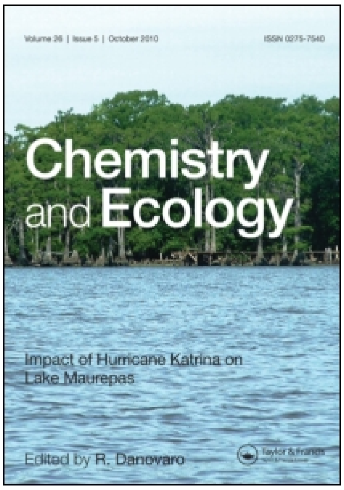

Chemistry and Ecology
Publication details, including instructions for authors and subscription information:
http://www.informaworld.com/smpp/title~content=t713455114

Rare earth elements distribution in seawater and suspended particulate of the Central Mediterranean Sea

P. Censi[a]; S. Mazzola[b]; M. Sprovieri[c]; A. Bonanno[b]; B. Patti[b]; R. Punturo[a]; S. E. Spoto[a]; F. Saiano[d]; G. Alonzo[d]
[a] Department of Geological Sciences, University of Catania, Catania, Italy [b] I.A.M.C. Geomare C.N.R., Naples, Italy [c] I.R.M.A. C.N.R., Mazara del Vallo (TP), Italy [d] I.T.A.F., University of Palermo, Palermo, Italy

To cite this Article Censi, P. , Mazzola, S. , Sprovieri, M. , Bonanno, A. , Patti, B. , Punturo, R. , Spoto, S. E. , Saiano, F. and Alonzo, G.(2004) 'Rare earth elements distribution in seawater and suspended particulate of the Central Mediterranean Sea', Chemistry and Ecology, 20: 5, 323 — 343

To link to this Article: DOI: 10.1080/02757540410001727954

URL: http://dx.doi.org/10.1080/02757540410001727954

Chemistry and Ecology
October 2004, Vol. 20(5), pp. 323–343

RARE EARTH ELEMENTS DISTRIBUTION IN SEAWATER AND SUSPENDED PARTICULATE OF THE CENTRAL MEDITERRANEAN SEA

P. CENSI[a], S. MAZZOLA[b,*], M. SPROVIERI[c], A. BONANNO[b], B. PATTI[b],
R. PUNTURO[a], S. E. SPOTO[a], F. SAIANO[d] and G. ALONZO[d]

[a]*Department of Geological Sciences, University of Catania, Catania, Italy;*
[b]*I.A.M.C. Geomare C.N.R., Naples, Italy;* [c]*I.R.M.A. C.N.R., Mazara del Vallo (TP), Italy;*
[d]*I.T.A.F., University of Palermo, Palermo, Italy*

(Received 30 June 2003; In final form 18 February 2004)

Rare earth element (REE) content in suspended and dissolved phases from the Strait of Sicily (Central Mediterranean Sea) has been measured. Vertical profiles of several dissolved REEs along the water column reflect the 3-D oceanographic features of the studied area and identifies the different water masses present there. Shale-normalized REE distribution patterns and derived parameters calculated for the suspended particulate show different atmospheric dust-surface inputs and their interactions with seawater. Finally, combined information from $[La/Yb]_N$, ratios, REE/La ratios and Eu anomalies measured in the suspended particulate suggest an important contribution of volcanic materials from the Etna volcano and Saharan dust to the lithogenic fraction of the suspended particulate.

Keywords: Rare earth elements; Strait of Sicily; Suspended particulate

1 INTRODUCTION

Rare earth elements (REE) enter the seawater budget primarily via atmospheric fallout (Elderfield and Greaves, 1982; De Baar *et al.*, 1983) and riverine inputs (Goldstein *et al.*, 1984; Frost *et al.*, 1986). Moreover, they exist essentially in the relative stable trivalent oxidation state and have a similar chemical behaviour, except for Ce and Eu, thus representing appropriate tracers for discriminating suspended particulate matter of different origins as authigenic, lithogenic and anthopogenic (Olmez *et al.*, 1990; Tachikawa *et al.*, 1999b).

The marine suspended particulate consists of an authigenic fraction, corresponding to the phases formed by *in situ* processes ($CaCO_3$, silica, organic matter, Mn–Fe oxyhydroxdes), a lithogenic fraction of terrigenous material (residual minerals, volcanic ejecta, clays minerals) and an anthropogenic fraction whose presence in seawater is common in areas located close to densely populated and highly industrial regions. Owing to the limited geographic area and the strict relationship with close continental areas, the epicontinental basins are eligible environments in which the effects of terrestrial material inputs in the seawater can be

---

[*] Corresponding author. E-mail: mazzola@irma.pa.cnr.it

ISSN 0275-7540 print; ISSN 1029-0370 online
DOI: 10.1080/02757540410001727954

monitored extensively. In the Mediterranean Sea, the deposition of atmospherically transported dust and mobilization of elements, by both wet and dry deposition, can play an important role in the chemistry of the water masses (Grousset *et al.*, 1990; Greaves *et al.*, 1991, 1994; Molinaroli, 1996; Güllü *et al.*, 2000; Elbaz-Poulichet *et al.*, 2001), especially in the important area of the Strait of Sicily where industrial activity is particularly well developed.

In this work, we present a detailed dataset of seawater and particulate REE concentrations from the central Mediterranean area (Strait of Sicily). The geographic distribution of the studied stations offers an opportunity to evaluate the REE distribution in a region in which the composition of seawater in terms of REE contents is not extensively monitored. Moreover, in the studied area, the riverine inputs can be reasonably neglected, thus allowing the opportunity to discern the effects of the atmospheric fallout and to evaluate the compositional signature of its different components.

The research has been planned to: (1) estimate variations of dissolved REEs in the Strait of Sicily related to seawater circulation in the Central Mediterranean area and (2) discern the different roles of lithogenic and anthropogenic fraction of suspended particulate using shale-normalized La/Yb ratios and the Eu anomaly (Eu/Eu*) as reliable proxies of different sources of suspended particulate in seawater. Actually, in the marine environment, fractionation processes that take place among the different REEs are different from those occurring under lithogenic conditions. Therefore, from the behaviour of REEs, normalized to the composition of residual rocks (*e.g.* shales), it is possible to distinguish the particulate fraction of authigenic origin, formed in the seawater, from the detritus fraction.

As a first approach, we estimate the enrichment of light REEs (LREE), from La to Gd, with respect to heavy REEs (HREE), from Tb to Lu. Such an approach is achieved here by monitoring the ratio between the shale-normalized La and Yb concentrations.

As a second approach, we calculate the enrichment or depletion of concentration of selected REE. Generally, Eu distribution is chosen because, under magmatic conditions, Eu^{2+} substitutes Ca^{2+} in eightfold coordination sites of the lattice structure in crystallizing plagioclase minerals (Hanson, 1989; McKay, 1989), while in the marine environment, Eu has a typical valency of 3+ like other REEs, except Ce. Therefore, a particulate fraction of lithogenic origin will show a positive Eu anomaly calculated according to the equation $Eu_n/Eu_n^* = 2[Eu]_n/([Sm]+[Gd])$ (De Baar *et al.*, 1985; Bertram and Elderfield, 1993), where $[Eu]_n$ is the shale-normalized REE, and Eu_n^* is the hypothetical shale-normalized Eu concentration calculated on its neighboring elements Sm and Gd.

2 MATERIAL AND METHODS

We have studied three different kinds of samples: (1) aerosol samples as source terms on atmospheric input in the basin, (2) seawater samples and (3) water-column suspended materials.

2.1 Aerosol Sampling

"Red dust" of atmospheric origin was collected using a polyethylene plate, with a surface area of 1 m^2, located at Mazara del Vallo in the western part of Sicily, close to Lilibeo Cape. Sample collections took place during October 1999, during a period free from precipitations during which large amounts of atmospheric "Red dust" were carried out under the action of the Sirocco wind. Pyroclastic materials ejected from the Etna volcano were collected in the same manner at Catania (Eastern Sicily) during the same "dry" period, during October 1999.

2.2 Sampling of Seawater and Suspended Particulate

Samples were collected in the early summer of 1999 during the JUVENILE 99 cruise, aboard the RV *Urania.* Figure 1 shows the location map of the stations where dissolved and particulate REE concentrations were measured.

The dissolved REE concentrations at the 10 stations together with the main hydrographic parameters (potential temperature and salinity) are listed in Tables I and II. Figure 2 shows the dissolved REE depth profiles of the selected stations S128, S455 and S626. The REE concentrations of particulate from water columns were measured at stations S24, S128, S455, S458 and S470 (Tabs. III and IV). Figure 3 shows the depth profiles of particulate REE concentrations for the selected stations S24, S128 and S455. Vertical sample spacing has been selected to emphasize the most important oceanographic discontinuities recorded by the salinity and temperature profiles (Fig. 2).

The sampling system consisted of a Neil–Brown CTD rosette frame and 24 × 12 l Teflon-lined GoFlo bottles. Upon recovery of the GoFlo bottles water samples were immediately filtered inside the shipboard through 0.4 μm Millipore® filters, using a Teflon tubing apparatus. Samples were acidified to pH 1–2 with HNO_3 Merck ULTRAPUR® and stored in hot-acid washed polyethylene bottles. In order to increase the signal-to-noise ratio in the studied seawaters 500 ml of each sample was pre-concentrated with CHELEX 100® (100–200 mesh) chelating resin:

- The pH value of each seawater sample was set to 6.0 with CH_3COONH_4 according to Möller *et al.* (1992), and an aliquot of each seawater sample passed on an 8 cm long column filled with CHELEX-100 100–200 mesh previously cleaned and conditioned according to Paulson (1986).
- REEs were eluted with 5 ml of HNO_3 3.5 M, giving a 100-fold enrichment factor. Details of the used procedures are reported in Paulson (1986) and Möller *et al.* (1992).

FIGURE 1 Location map of the sampling stations. ■: sampling stations where both seawater and suspended particulate were analysed; ●: sampling stations where only seawater was analysed.

TABLE I Station names, sampling depths, physical-chemical parameters of the water columns, REE concentrations (pmol/l) and values of the Eu anomalies in seawater samples from stations located in the Ionian sea.

Station	*Depth (m)*	*Temperature (°C)*	*Salinity (‰)*	*La*	*Ce*	*Pr*	*Nd*	*Sm*	*Eu*	*Gd*	*Tb*	*Dy*	*Ho*	*Er*	*Tm*	*Yb*	*Lu*	*Eu/Eu**
S-A24	20	23.55	38.62	23.51	17.51	4.49	22.47	5.16	1.45	7.69	1.33	9.45	2.61	8.02	1.12	7.54	1.06	1.13
	55	23.62	38.51	23.60	15.64	4.08	20.36	4.56	1.37	7.20	1.21	9.15	2.52	7.29	1.09	7.07	0.99	0.92
	100	22.42	38.65	23.30	14.60	3.98	20.48	4.60	1.44	7.47	1.24	9.26	2.57	7.34	1.09	7.09	0.98	0.96
	250	17.83	38.80	24.05	14.83	4.58	25.06	5.25	1.58	8.06	1.39	9.10	2.69	7.43	1.12	7.22	1.06	1.01
	300	17.00	38.81	24.13	15.90	4.63	23.86	5.09	1.50	7.83	1.40	9.41	2.78	7.93	1.18	7.37	1.06	1.17
	375	16.11	38.78	23.11	15.36	4.83	24.52	5.16	1.54	7.97	1.37	9.58	2.78	7.86	1.17	7.34	1.05	1.23
	450	15.46	38.78	24.13	16.25	4.63	24.40	5.15	1.44	8.28	1.41	9.54	2.78	7.90	1.18	7.35	1.03	1.25
	525	15.03	38.78	24.73	15.86	4.83	25.36	5.32	1.50	8.17	1.34	9.56	2.57	7.72	1.22	7.45	1.04	1.20
S-46	20	0.24	38.67	25.76	18.67	4.85	23.61	5.34	1.60	7.94	1.47	10.33	2.97	8.74	1.15	7.29	1.15	1.11
	35	24.06	38.67	24.30	16.69	4.71	22.71	5.12	1.42	7.75	1.42	10.20	2.89	8.51	1.10	7.22	1.12	1.00
	40	24.08	38.32	24.05	16.33	4.51	22.00	4.87	1.44	7.32	1.37	10.04	2.88	8.25	1.12	7.15	1.09	0.96
	50	24.11	38.35	24.05	15.99	4.61	21.45	5.00	1.41	7.47	1.41	9.84	2.68	8.05	1.15	7.75	1.13	0.93
	55	24.07	38.37	24.22	15.99	4.39	21.08	4.91	1.40	7.11	1.36	9.53	2.79	8.30	1.13	7.26	1.12	0.94
	65	23.89	38.51	24.73	15.90	4.53	20.96	4.99	1.40	7.27	1.38	9.66	2.63	8.30	1.11	7.47	1.07	0.98
	75	23.51	38.51	23.70	15.23	4.40	21.57	4.98	1.40	7.64	1.28	9.80	2.43	8.51	1.16	7.02	1.11	1.01
S-196	15	26.24	38.32	28.50	20.70	5.51	27.00	5.80	1.86	9.03	1.68	9.95	2.76	9.39	1.38	7.85	1.29	1.09
	20	26.18	38.38	27.13	18.33	5.19	24.70	5.64	1.59	8.67	1.59	9.63	2.81	9.61	1.36	7.60	1.25	1.00
	35	26.06	37.65	25.93	17.87	5.05	24.16	5.38	1.49	8.31	1.56	9.70	2.82	8.97	1.34	7.15	1.18	1.07
	50	25.84	37.87	25.59	17.84	5.02	23.73	5.44	1.53	8.00	1.53	9.72	2.81	9.01	1.33	7.08	1.18	1.03
	60	25.58	38.56	24.73	17.59	5.08	23.80	5.45	1.48	8.00	1.51	9.76	2.79	9.06	1.32	7.53	1.21	1.06
	75	25.03	38.57	24.30	18.14	4.92	23.73	5.48	1.46	7.72	1.56	9.63	2.69	8.86	1.34	7.98	1.13	1.04
	95	24.02	38.64	25.07	17.65	5.10	24.82	5.36	1.45	7.78	1.49	9.76	2.87	8.85	1.39	7.10	1.18	1.00
S-470	10	25.90	37.92	30.78	22.48	6.19	31.39	6.58	1.99	9.53	1.88	11.23	3.19	10.22	1.32	9.01	1.41	0.91
	42	25.58	37.61	29.18	20.31	5.88	28.85	5.90	1.63	9.20	1.73	11.02	2.99	9.85	1.27	9.00	1.26	0.91
	55	25.19	37.68	27.81	19.17	5.54	28.57	5.69	1.65	8.42	1.70	10.70	2.96	9.68	1.24	8.87	1.20	0.91
	70	24.54	37.98	25.84	19.27	5.60	27.08	5.62	1.64	8.36	1.60	10.70	2.89	9.54	1.23	8.82	1.26	1.06
	85	23.78	37.94	25.93	19.37	5.40	27.51	5.72	1.59	8.22	1.60	10.46	2.89	9.60	1.26	8.83	1.19	1.15
	100	22.97	38.17	25.93	18.72	5.56	27.43	5.85	1.61	8.20	1.57	10.40	3.17	9.65	1.24	8.57	1.23	1.15
	115	21.67	38.27	27.39	20.10	5.75	26.44	5.65	1.60	8.25	1.62	10.48	3.01	9.50	1.27	8.45	1.23	1.10

TABLE II Station names, sampling depths, physical-chemical parameters of the water columns, REE concentrations (pmol/l) and values of the Eu anomalies in seawater samples from stations located in the Strait of Sicily.

Station	*Depth (m)*	*Temperature (°C)*	*Salinity (‰)*	*La*	*Ce*	*Pr*	*Nd*	*Sm*	*Eu*	*Gd*	*Tb*	*Dy*	*Ho*	*Er*	*Tm*	*Yb*	*Lu*	*Eu/Eu**
S-626	15	25.33	37.86	25.20	15.74	4.25	22.00	4.71	1.49	8.38	1.35	8.91	2.11	7.26	1.03	7.78	1.15	1.17
	35	25.32	37.42	20.72	13.79	4.07	19.59	4.64	1.27	7.76	1.24	7.80	2.02	7.03	0.97	7.51	1.05	1.04
	65	24.86	37.85	21.60	12.80	4.02	19.94	4.89	1.22	7.76	1.16	7.38	2.08	6.89	0.96	7.36	1.05	1.06
	125	22.34	38.47	21.18	12.50	4.15	20.43	4.99	1.23	7.69	1.19	7.35	1.99	6.94	0.90	7.18	1.03	1.10
	230	18.72	38.74	21.26	12.07	4.33	22.41	4.64	1.29	7.57	1.22	7.43	1.87	7.06	1.02	7.41	1.06	0.98
	280	17.67	38.77	22.34	11.21	4.20	23.12	4.85	1.33	7.74	1.21	7.46	1.92	7.33	1.05	7.44	0.98	1.03
	360	16.51	38.76	23.00	11.69	4.36	23.33	4.97	1.34	7.45	1.32	8.38	1.94	7.77	1.08	7.52	0.97	0.99
	450	15.67	38.76	24.23	11.16	4.33	21.49	5.00	1.25	7.67	1.35	8.21	1.91	7.66	1.09	7.61	1.03	1.00
	510	15.23	38.75	23.91	12.60	4.57	21.35	4.92	1.32	7.81	1.36	9.08	1.86	7.71	1.09	7.62	1.08	1.02
S-464	20	23.19	37.78	28.13	20.37	4.54	27.79	5.82	1.53	8.91	1.63	8.40	2.27	7.43	1.02	8.19	1.14	0.88
	45	23.41	37.61	26.23	18.18	4.74	24.54	5.47	1.38	8.11	1.52	8.00	2.18	7.22	0.97	7.83	1.08	0.87
	65	23.22	37.58	24.23	17.84	4.64	25.45	5.18	1.36	8.04	1.45	7.77	2.20	7.66	0.98	7.75	1.08	1.12
	110	21.80	38.17	23.42	17.70	4.70	23.76	5.13	1.35	8.02	1.48	7.57	2.08	7.61	0.96	7.68	1.06	1.05
	180	19.53	38.65	25.00	17.18	4.59	25.17	4.83	1.34	8.19	1.50	7.57	2.04	7.24	0.96	7.74	1.04	1.09
	230	18.30	38.74	26.06	17.13	4.46	25.81	5.04	1.44	8.22	1.42	8.19	2.23	7.66	0.98	7.81	1.09	0.95
	290	17.18	38.78	27.39	17.84	4.77	26.00	5.20	1.52	8.24	1.59	7.82	1.81	7.73	0.96	7.88	1.11	0.97
	370	16.18	38.77	26.23	18.56	4.87	25.88	5.10	1.41	8.13	1.59	8.00	2.08	7.57	0.95	7.81	1.09	0.96
	450	15.51	38.77	25.73	19.37	5.18	26.80	5.31	1.56	8.31	1.64	8.10	2.05	7.94	0.99	7.83	1.08	0.98
S-458	15	23.87	37.83	27.64	19.27	5.54	26.68	5.72	1.79	8.61	1.53	10.64	2.67	9.24	1.15	8.43	1.16	0.94
	35	24.09	37.39	24.33	17.60	5.25	25.65	4.71	1.57	8.02	1.48	10.25	2.64	8.80	1.21	8.38	1.07	0.92
	60	24.04	37.64	17.72	17.04	5.13	25.18	5.25	1.45	7.90	1.40	10.15	2.58	8.60	1.04	8.28	1.14	0.93
	115	22.05	38.25	23.00	15.55	5.03	26.44	4.94	1.37	7.88	1.37	9.32	2.19	8.68	1.01	8.06	1.12	0.93
	150	20.66	38.52	23.17	15.41	5.18	27.15	5.00	1.37	8.29	1.43	9.58	2.19	8.26	1.04	8.13	1.09	0.93
	250	17.78	38.75	25.73	15.55	5.02	27.79	4.78	1.38	8.45	1.51	10.06	2.32	8.60	0.99	8.13	1.13	0.98
	330	16.51	38.77	24.57	17.03	5.00	27.36	4.94	1.46	8.45	1.53	10.28	2.19	8.68	0.98	8.13	1.15	1.02
	360	16.18	38.77	24.74	16.46	5.03	27.29	4.74	1.47	8.27	1.57	9.91	2.14	8.52	0.98	8.17	1.15	0.96
	400	15.83	38.77	24.91	18.23	4.64	28.28	4.90	1.32	8.63	1.59	10.13	2.14	8.89	0.92	8.25	1.13	1.03
	560	14.92	38.76	26.23	17.37	5.08	29.20	4.72	1.34	9.05	1.69	9.80	2.10	9.03	1.03	8.21	1.13	1.13
S-455	15	24.14	37.85	25.90	18.46	4.84	25.31	5.21	1.62	7.94	1.44	9.50	2.66	8.15	1.25	8.48	1.22	1.04
	45	24.26	37.46	23.17	16.56	4.40	23.19	4.72	1.46	7.76	1.28	9.29	2.26	7.64	1.15	8.41	1.15	1.02
	140	20.38	38.63	21.26	14.55	4.40	22.70	4.47	1.49	7.78	1.26	8.00	2.26	7.38	1.10	8.18	1.07	0.92

(*continued*)

TABLE II Continued.

Station	*Depth (m)*	*Temperature (°C)*	*Salinity (‰)*	*La*	*Ce*	*Pr*	*Nd*	*Sm*	*Eu*	*Gd*	*Tb*	*Dy*	*Ho*	*Er*	*Tm*	*Yb*	*Lu*	Eu/Eu^*
	185	18.77	38.73	24.33	14.17	4.36	24.61	4.64	1.31	7.85	1.28	8.05	2.45	7.50	1.19	8.24	1.16	0.87
	250	17.24	38.76	25.07	14.74	4.25	24.54	4.69	1.36	7.94	1.35	9.08	2.42	7.97	1.20	8.24	1.19	0.88
	300	16.55	38.78	24.66	14.17	4.51	24.11	4.89	1.37	7.94	1.28	9.05	2.48	7.97	1.26	8.31	1.22	0.95
	380	15.80	38.77	23.25	15.00	4.59	24.75	4.69	1.37	7.90	1.28	9.05	2.40	8.74	1.26	8.49	1.21	0.95
	515	14.98	38.76	24.41	14.50	4.74	24.96	4.47	1.28	8.10	1.31	9.76	2.44	8.60	1.20	8.51	1.17	0.98
	575	14.73	38.75	24.24	13.60	4.82	26.09	4.79	1.33	8.33	1.37	9.60	2.49	8.40	1.22	8.39	1.12	0.89
	650	14.56	38.75	24.82	12.93	4.75	25.53	4.63	1.30	8.18	1.25	9.52	2.58	8.54	1.30	8.39	1.22	0.93
S-290	20	23.79	37.97	27.85	17.76	5.19	24.14	5.55	1.65	8.51	1.76	11.13	3.00	9.74	1.28	8.38	1.24	1.13
	50	23.82	37.72	25.08	16.71	4.54	22.00	4.55	1.59	7.84	1.22	10.22	2.81	8.16	1.23	7.93	1.14	1.01
	95	22.27	38.37	25.32	16.05	4.21	21.79	4.41	1.57	7.83	1.33	8.92	2.68	8.09	1.04	7.70	1.07	0.98
	235	17.76	38.76	20.87	14.61	4.46	23.15	4.80	1.53	7.76	1.51	9.34	2.67	8.43	1.15	7.40	1.07	1.03
	300	16.66	38.78	21.60	14.30	4.50	25.31	4.69	1.61	7.71	1.46	9.60	2.62	8.60	1.10	7.45	1.22	0.99
	350	15.68	38.77	22.63	15.93	4.69	26.05	4.93	1.52	8.25	1.59	9.18	2.80	8.66	1.11	7.47	1.20	1.00
	400	16.11	38.70	23.22	16.00	4.76	24.88	4.81	1.50	7.95	1.46	9.64	2.29	8.86	1.11	7.77	1.11	1.00
	450	15.37	38.77	23.47	16.32	4.86	23.46	4.96	1.56	7.83	1.49	9.38	2.66	8.77	1.12	7.80	1.20	1.12
	500	15.10	38.77	24.90	15.93	4.74	23.27	5.08	1.45	8.23	1.40	9.11	2.51	9.11	1.10	7.72	1.14	0.98
	575	14.80	38.76	25.08	16.20	4.80	22.41	4.98	1.51	8.16	1.37	9.28	2.57	8.83	1.12	7.74	1.20	1.06
	660	14.54	38.75	24.57	16.82	4.93	20.06	5.15	1.44	8.02	1.29	9.28	2.53	8.83	1.10	7.93	1.22	1.06
	740	14.36	38.74	25.07	15.66	4.71	20.06	5.15	1.52	8.47	1.54	9.18	2.47	8.66	1.00	7.77	1.19	1.03
	860	14.17	38.74	25.16	17.20	4.93	19.94	5.32	1.52	8.14	1.56	9.48	2.41	8.21	1.12	7.70	1.15	1.04
S-128	15	22.57	37.91	25.46	12.67	4.51	27.96	4.84	1.59	7.79	1.58	11.77	2.84	10.61	1.21	7.56	0.89	1.02
	25	22.65	37.92	23.95	13.76	4.11	26.67	4.97	1.34	8.16	1.73	12.40	3.15	10.27	1.28	7.72	1.02	1.05
	40	22.76	37.86	25.08	13.26	3.94	25.68	4.51	1.34	8.03	1.51	10.60	3.08	10.27	1.33	7.49	1.05	1.08
	70	22.13	38.13	22.88	13.12	4.19	25.12	4.34	1.41	8.11	1.49	9.99	3.08	9.28	1.12	7.42	1.02	1.07
	105	20.77	38.49	23.95	12.44	4.06	25.80	4.44	1.66	8.26	1.48	9.85	2.64	8.67	1.27	7.15	0.99	1.05
	125	20.02	38.57	22.28	12.52	4.14	24.51	4.44	1.74	8.27	1.51	9.23	2.67	8.37	1.15	7.56	1.07	1.06
	140	19.51	38.61	22.88	11.86	4.21	25.74	4.36	1.74	8.18	1.49	9.54	2.73	8.97	1.24	6.93	1.02	0.97
	162	18.66	38.62	23.29	12.09	4.19	23.89	4.22	1.64	8.00	1.60	10.30	2.82	9.57	1.19	7.31	1.11	1.00

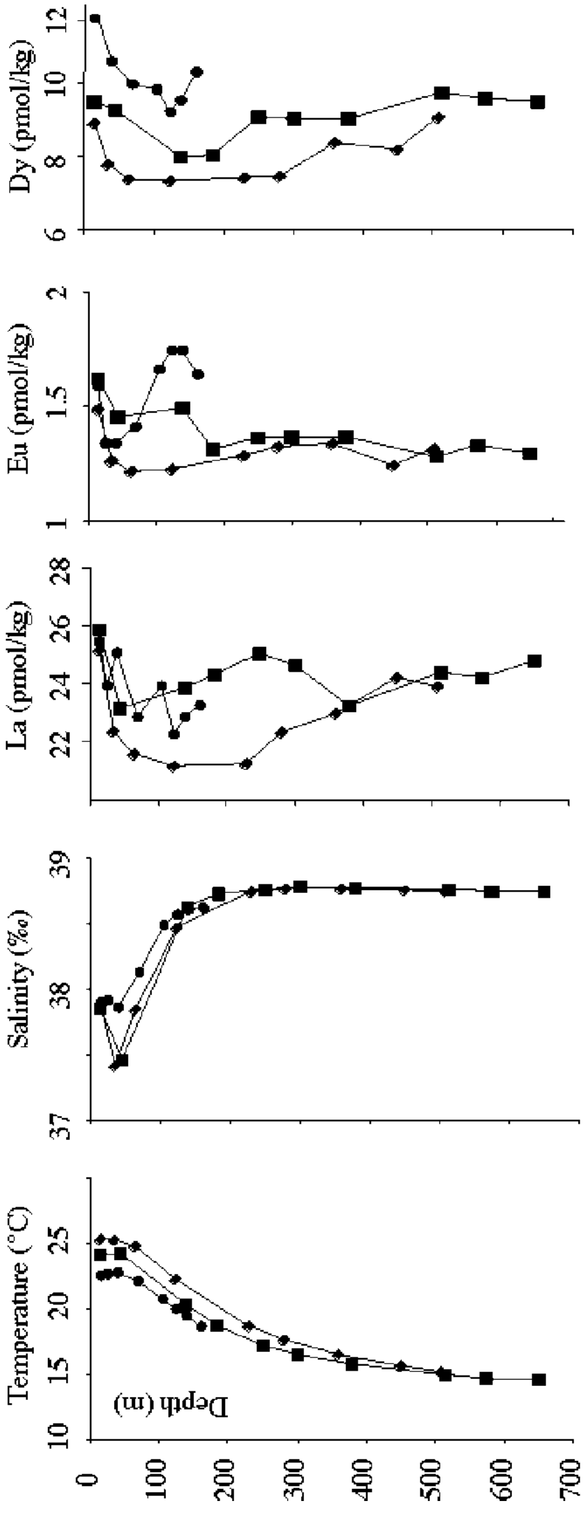

FIGURE 2 Profiles of more representative REE contents along the water column in selected stations. Concentration values for all the REE are reported in pmol/l. ◆: S-626; ■: S-455; ●: S-128.

TABLE III Station names, sampling depths, REE concentrations (μg/kg), Ce and Eu anomalies, shale-normalized La/Yb ratios in suspended particulate from seawater (samples from stations located in the Ionian Sea).

Station	*Depth (m)*	*La*	*Ce*	*Pr*	*Nd*	*Sm*	*Eu*	*Gd*	*Tb*	*Dy*	*Ho*	*Er*	*Tm*	*Yb*	*Lu*	*Eu/Eu**	*[La/Yb]N*
S-24	20	513.52	762.29	107.62	397.77	56.48	13.25	47.42	7.43	40.38	5.84	17.43	2.52	12.91	2.29	1.21	2.94
	100	382.00	443.35	38.06	201.58	62.63	12.42	51.48	7.78	35.55	5.94	15.05	2.45	13.13	1.64	1.03	2.15
	250	515.30	1687.57	197.44	672.33	75.15	15.75	73.09	8.77	47.61	6.58	21.82	2.46	14.85	2.50	1.00	2.56
	300	156.76	509.04	36.45	188.15	61.83	13.72	50.14	8.20	39.54	7.43	19.23	2.86	16.00	2.52	1.16	0.72
	375	67.52	222.20	22.24	133.46	45.56	9.59	34.21	5.38	26.37	4.13	14.95	1.98	10.29	1.56	1.14	0.48
	450	60.94	286.25	24.42	102.41	40.76	12.25	36.68	6.99	29.98	5.04	15.87	2.42	13.07	2.82	1.49	0.34
	525	87.11	344.15	26.21	133.18	46.73	7.97	45.90	5.42	32.17	4.90	16.05	2.10	11.10	1.24	0.81	0.58
S-470	10	109.39	313.87	21.23	77.92	27.20	8.07	33.58	4.19	18.05	5.72	17.76	2.22	14.78	1.48	1.23	0.55
	42	34.26	212.20	16.55	59.14	15.06	3.76	17.55	2.60	15.59	6.60	16.17	2.55	13.82	1.00	1.07	0.18
	55	49.14	150.23	17.75	75.59	22.78	4.70	20.70	2.42	17.75	7.50	17.45	2.02	14.47	1.17	1.02	0.25
	70	92.20	232.68	7.81	41.47	8.98	4.68	17.27	3.19	16.22	7.26	18.28	2.38	14.47	1.09	1.63	0.47
	85	139.13	395.14	25.57	61.56	11.11	3.94	12.50	3.00	17.59	8.88	18.32	2.41	12.32	1.08	1.56	0.83
	100	492.11	669.88	61.03	181.82	32.71	6.67	27.45	3.28	20.96	7.35	18.88	2.84	13.20	1.07	1.05	2.75
	115	92.40	125.66	13.11	53.53	15.30	4.69	18.43	4.06	21.76	6.49	18.96	2.60	13.20	1.05	1.29	0.52

TABLE IV Station names, sampling depths, REE concentrations (μg/kg), Ce and Eu anomalies, shale-normalized La/Yb ratios in suspended particulate from seawater (samples from stations located in the Strait of Sicily).

Station	*Depth (m)*	*La*	*Ce*	*Pr*	*Nd*	*Sm*	*Eu*	*Gd*	*Tb*	*Dy*	*Ho*	*Er*	*Tm*	*Yb*	*Lu*	*Eu/Eu**	*[La/Yb]N*
S-455	15	597.44	943.65	111.19	277.73	22.81	4.34	19.16	2.55	26.65	6.05	19.47	2.13	6.67	1.04	0.98	6.61
	45	89.53	533.03	92.84	309.03	27.83	6.59	20.45	3.04	16.24	6.30	19.08	2.71	7.44	1.22	1.30	0.89
	140	30.04	160.97	19.40	95.35	15.30	6.83	16.20	2.82	15.41	6.78	18.11	2.41	6.80	1.05	2.03	0.33
	185	530.43	472.63	79.39	310.98	30.11	6.65	25.80	3.00	12.51	7.63	17.92	2.84	7.50	1.27	1.12	5.22
	250	138.71	292.92	47.61	84.91	13.87	3.34	12.48	1.91	16.10	4.74	15.19	2.75	6.86	0.97	1.19	1.49
	300	428.61	423.25	78.59	258.75	39.15	7.90	34.48	5.10	28.01	3.81	11.88	2.83	9.54	1.56	1.01	3.32
	380	1461.43	2356.10	276.79	841.11	57.02	8.64	37.18	4.83	22.96	5.13	17.99	3.19	7.47	1.00	0.88	14.44
	515	650.09	605.15	139.71	541.66	120.40	27.53	107.97	16.56	74.53	14.22	37.63	5.06	25.25	4.86	1.14	1.90
	575	1808.76	2401.46	300.66	1308.19	157.92	36.12	153.92	22.30	118.63	20.92	52.86	6.61	38.76	6.20	1.09	3.44
	650	2879.83	4806.60	612.23	1865.05	107.66	25.79	144.71	16.89	77.86	13.73	37.61	4.49	28.46	3.53	0.95	7.47
S-458	15	367.18	826.22	54.64	238.34	31.24	6.15	19.18	3.04	18.65	5.14	20.75	2.73	12.32	1.83	1.17	2.20
	35	637.64	1200.00	123.29	355.67	44.32	11.39	31.10	3.05	18.43	3.94	19.48	2.55	13.50	1.93	1.44	3.49
	60	2280.00	3939.99	432.77	931.79	101.09	16.73	37.54	4.73	20.16	4.01	19.83	2.74	16.61	1.64	1.18	10.13
	115	561.52	1054.25	97.25	344.68	50.60	7.32	28.52	2.42	20.49	4.13	19.64	2.82	14.81	1.89	0.89	2.80
	150	600.82	1078.16	96.43	373.84	47.24	6.68	22.76	2.97	14.48	3.58	17.86	2.90	14.14	1.78	0.92	3.14
	250	1250.00	2100.11	223.97	805.72	123.01	16.97	68.25	10.60	45.97	7.81	19.15	2.80	15.87	1.65	0.85	5.82
	330	2360.00	3312.08	343.57	1247.91	132.95	23.14	104.44	16.98	81.27	13.10	28.46	2.71	17.84	2.76	0.92	9.77
	360	695.78	1347.39	143.33	589.46	94.82	18.36	88.33	9.77	56.37	8.26	13.64	2.50	15.87	2.15	0.94	3.24
	400	2130.00	3380.15	346.43	1300.97	198.97	27.90	203.61	27.16	138.99	26.99	54.64	6.23	37.61	3.43	0.65	4.18
	560	3050.00	4830.00	1006.57	4000.35	790.13	158.88	760.42	91.66	626.08	93.41	140.86	12.78	69.25	9.01	0.96	3.25
S-128	15	1170.00	1780.37	198.51	767.30	153.65	35.81	141.06	21.91	110.97	17.88	47.12	5.33	39.41	3.97	1.14	2.19
	25	199.97	347.17	47.50	179.56	43.12	11.31	34.43	4.95	26.03	4.61	11.99	1.65	9.32	1.24	1.38	1.58
	40	366.23	537.99	61.75	183.86	45.15	12.12	34.73	3.42	22.22	4.79	11.19	1.43	7.88	0.93	1.44	3.43
	70	178.49	289.04	35.52	169.56	41.18	9.41	28.37	4.01	22.12	5.28	13.77	1.72	8.14	1.09	1.29	1.62
	105	1610.00	2007.10	246.86	943.78	196.80	44.81	181.57	26.91	139.18	23.16	64.55	9.05	49.57	6.23	1.11	2.40
	125	3090.00	5090.00	795.77	3302.21	708.35	163.39	652.35	93.22	493.94	86.53	219.01	25.75	158.84	21.12	1.13	1.44
	140	4760.00	7455.15	950.95	3829.14	770.77	171.41	731.38	101.57	541.47	98.11	233.85	28.46	174.15	22.36	1.07	2.02
	162	4250.00	6901.17	849.56	3299.35	657.47	154.76	630.94	83.92	465.50	81.14	203.62	24.67	148.58	20.31	1.13	2.11

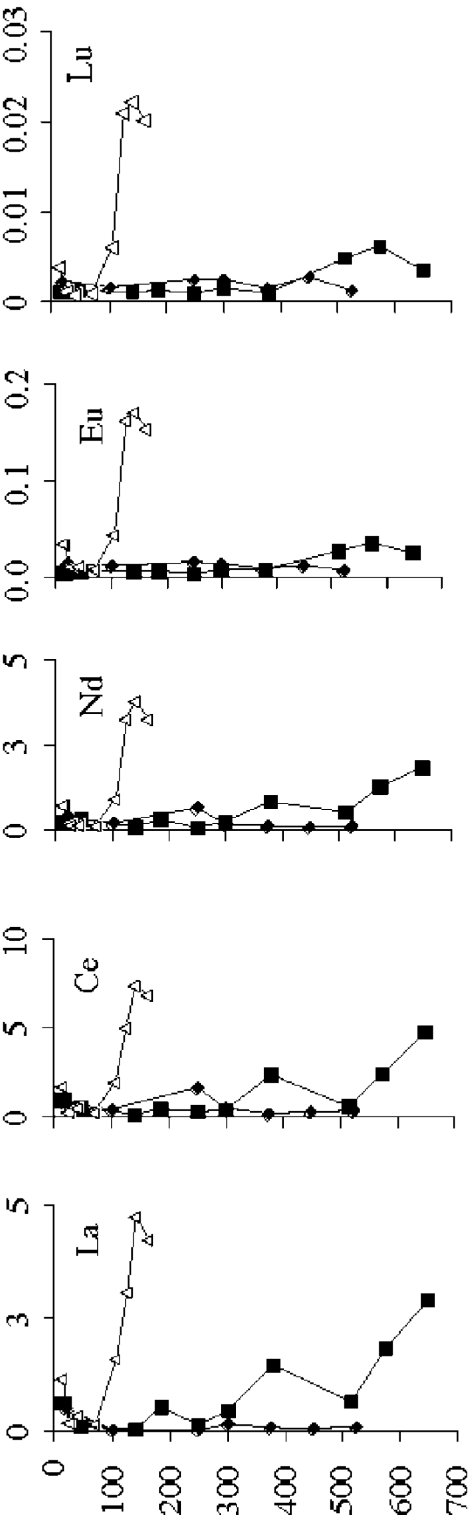

FIGURE 3 Profiles of more representative REE contents in particulate matter from seawater samples of selected stations. Concentration values for all the REE are reported in μg/kg. ◆: S-24; ■: S-455; △: S-128.

2.3 Analytical Methodologies

REE recovery and accuracy were monitored using about 10 l of an artificially prepared seawater standard solution. This was treated as a normal seawater sample, and its trace-element contents were removed using an 8 cm long column filled with CHELEX-100 100–200 mesh, as reported above. Such a procedure was repeated five times to ensure that all original trace-element contents from seawater were removed. Then, 10 ppt of REY was added to the seawater free from traces, and the resulting standard solution (AAPS in Tab. V) was pre-concentrated with CHELEX 100®. The recovery procedures were repeated five times (EL-1, EL-2, EL-3, EL-4 and EL-5). The resulting concentration values, their aritmethic averages and standard deviations are listed in Table V. The eluted fractions, for both samples and standard solutions, were analysed with an high-resolution ICP-MS (Thermo-FinniganMAT Element 2) using 100 ppt Rh as internal standard. The measurements were carried out in high-resolution mode, allowing the signal of the elements to be separated from those of most isobaric interferences as BaO^+.

Analytical blanks were obtained with 50 ml of HNO_3 Merck Ultrapure in Millipore ultrapure waters, and concentrations were negligible compared with measured REE concentrations. Five aliquots of this ultrapure solution were analysed five times and the standard deviations calculated from the average values measured (Tab. V). Detection limits are evaluated as three times the standard deviations measured for analytical blanks according to Barbante *et al.* (1999) and are listed in Table V.

To evaluate the contribution of REE released from CHELEX-100 and chemicals used during concentration procedures, a set of five blanks (PB-1, PB-2, PB-3, PB-4 and PN-5) was prepared using Millipore ultrapure water with the same quantities of all chemicals used to concentrate REE from seawater. The results are listed in Table V.

For complete dissolution, a number of acids were chosen for sample digestion. All reactants were from Merck® and of "Ultrapure" quality: hydrochloric acid (37% v/v), nitric acid (65% v/v), and hydrofluoric acid (48% v/v). Water was prepared using bidistilled water with a Millipore® MilliQ apparatus (18.2 Mohm/cm). The high-pressure digestion device used here is a Mars5 microwave oven (CEM Technologies). Twelve samples can be digested per run. The instrument is provided with a high-pressure and temperature controller. The microwave digestion procedure offers relatively quick digestion and complete dissolution of refractory minerals. First, particulate matter (about 0.015 g) was collected on a millipore filter (pore size 0.4 μm) from seawater (approximately 6 l) that was acidified after filtration to collect both the labile "authigenic" fraction and the detritus "lithogenic" fraction on the filter (FengFu *et al.*, 1997). Then, suspended matter was weighed with a 0.01 mg analytical balance and placed into the tetrafluormethaxyl (TFM) digestion container with the filter. An acid solution was added, with the following acid ratio: $HCl:HNO_3:HF = 4:4:4$ (total volume = 12 ml). The containers were carefully sealed, placed into the carousel and heated with 100% power (1200 W), with a pressure ramp of 30′, and then maintained at stable pressure and temperature conditions ($T = 220\,^{\circ}C$; $P = 400$ psi) for 2 h.

After complete dissolution, excess acid was removed up to incipient dryness using a CEM microvap™ apparatus, 5 ml of nitric acid (65% v/v) was added, and the sample solutions were diluted to 100 ml with Millipore® water and transferred into previously cleaned 100 ml polycarbonate bottles.

Ten different procedural blanks obtained by complete dissolution of five different filters (MF-1, MF-2, MF-3, MF-4, MF-5) were carried out according to the above mentioned procedure to evaluate the trace-element contents in the filters and other chemicals used. The results are listed in Table VI.

TABLE V Measured mass, average of five different determinations of analytical blank concentrations (Bl.conc), related standard deviations, detection limits of analyses, elemental concentrations both in procedural blanks (PB-1, PB-2, PB-3, PB-4, PB-5), in artificially prepared seawater standard (APSS) and eluted fractions (EL-1, EL-2, EL-3, EL-4, EL-5) and related recovery values measured.

		Analytical blank			*Procedural blank*								*Standard concentration*					*Recovery*						
		Bl.conc.	$\pm\sigma$	*D.L.*	*PB-1*	*PB-2*	*PB-3*	*PB-4*	*PB-5*	*Mean*	$\pm\sigma$	*APSS*	*EL-1*	*EL-2*	*EL-3*	*EL-4*	*EL-5*	*EL-1*	*EL-2*	*EL-3*	*EL-4*	*EL-5*	*Mean*	$\pm\sigma$
139	La	0.83	0.12	0.36	0.91	0.96	1.10	1.07	1.11	1.03	0.09	112.5	101.8	105.7	104.6	105.7	102.5	90.5	94.0	93.0	93.9	91.2	92.5	1.6
140	Ce	0.35	0.18	0.53	0.42	0.91	0.92	0.99	1.03	0.86	0.25	72.0	68.5	66.5	69.2	66.4	66.9	95.1	92.4	96.1	92.3	92.9	93.8	1.7
141	Pr	0.08	0.01	0.04	0.21	1.01	1.16	1.13	1.16	0.94	0.41	71.4	69.4	66.9	72.2	65.8	68.9	97.3	93.8	101.1	92.2	96.6	96.2	3.4
143	Nd	0.20	0.06	0.18	0.17	1.18	0.91	0.93	0.91	0.82	0.38	71.0	64.3	65.5	62.4	64.2	64.1	90.7	92.3	88.0	90.5	90.4	90.4	1.5
154	Sm	0.09	0.05	0.15	0.16	1.15	1.09	0.94	1.07	0.88	0.41	69.3	64.0	65.8	63.5	66.3	66.8	92.3	94.9	91.5	95.7	96.4	94.2	2.1
153	Eu	0.05	0.02	0.05	0.08	1.11	1.02	1.16	1.11	0.90	0.46	66.5	64.4	65.4	64.9	61.4	61.8	96.8	98.4	97.6	92.3	92.9	95.6	2.8
155	Gd	0.31	0.15	0.46	0.07	1.06	0.98	1.05	0.91	0.81	0.42	65.8	59.3	61.5	61.1	57.6	60.0	90.2	93.4	92.8	87.6	91.1	91.0	2.3
159	Tb	0.22	0.13	0.40	0.09	1.13	1.11	1.11	0.90	0.87	0.45	63.6	58.4	56.7	57.3	55.4	58.2	91.8	89.2	90.1	87.0	91.5	89.9	1.9
164	Dy	0.30	0.05	0.14	0.11	1.05	1.10	0.97	0.98	0.84	0.41	62.9	58.6	60.7	59.1	57.4	60.9	93.1	96.4	93.9	91.2	96.7	94.3	2.3
165	Ho	0.48	0.19	0.56	0.08	0.96	1.08	1.06	1.14	0.86	0.44	61.5	57.8	59.5	54.7	58.0	59.6	93.9	96.6	88.9	94.3	96.8	94.1	3.2
168	Er	0.07	0.04	0.12	0.06	0.91	1.16	1.00	0.96	0.82	0.43	60.6	56.7	54.3	57.8	53.7	54.3	93.5	89.6	95.4	88.6	89.5	91.3	3.0
169	Tm	0.02	0.01	0.02	0.05	1.03	0.96	0.97	1.14	0.83	0.44	59.8	54.6	52.0	54.2	54.3	49.2	91.4	86.9	90.6	90.8	82.2	88.4	3.9
174	Yb	0.03	0.01	0.02	0.04	0.96	0.99	0.92	1.06	0.79	0.42	59.2	54.6	56.4	56.0	53.4	57.1	92.3	95.2	94.5	90.2	96.4	93.7	2.5
175	Lu	0.02	0.01	0.02	0.07	1.04	1.17	0.94	1.00	0.84	0.44	57.2	54.0	53.6	51.4	51.0	54.5	94.5	93.9	89.9	89.3	95.4	92.6	2.8

Note: All the concentration values are given in pmol/l. For detailed explanations see text.

TABLE VI Used masses, measured REE concentrations in standard reference materials compared with certified values from Govindaraju (1994) and in five different mineralized filters, mean values and standard deviations.

		MAG Meas. mg/kg	*MAG REF.* *mg/kg*	*AGV Meas.* *mg/kg*	*AGV REF.* *mg/kg*	*BHVO Meas.* *mg/kg*	*BHVO REF.* *mg/kg*	*MF-1* *g/kg*	*MF-2* *g/kg*	*MF-3* *g/kg*	*MF-4* *g/kg*	*MF-5* *g/kg*	*Mean* *g/kg*	$\pm\sigma$ *g/kg*
139	La	45.99	43.00	1218.04	1226.00	127.10	139.00	6.879	6.301	6.872	6.604	7.269	6.785	0.360
140	Ce	93.11	88.00	38.85	38.00	15.18	15.80	9.143	10.395	9.022	9.001	9.521	9.417	0.585
141	Pr	9.27	9.30	67.49	67.00	36.70	39.00	1.303	1.511	1.518	1.228	1.179	1.348	0.158
143	Nd	38.66	38.00	7.96	7.60	5.35	5.70	5.626	5.659	6.501	5.159	5.825	5.754	0.486
154	Sm	7.94	7.50	30.86	33.00	23.48	25.20	0.059	0.070	0.056	0.059	0.061	0.061	0.005
153	Eu	1.66	1.55	5.82	5.90	5.74	6.20	0.353	0.364	0.339	0.322	0.396	0.355	0.028
155	Gd	6.25	5.80	1.62	1.64	1.92	2.06	0.029	0.034	0.031	0.029	0.030	0.031	0.002
159	Tb	0.95	0.96	5.92	5.00	5.92	6.40	0.062	0.071	0.064	0.066	0.067	0.066	0.003
164	Dy	5.20	5.20	0.74	0.70	0.86	0.96	0.117	0.126	0.111	0.108	0.129	0.118	0.009
165	Ho	1.09	1.02	3.57	3.60	4.82	5.20	0.268	0.304	0.274	0.289	0.273	0.282	0.015
168	Er	3.13	3.00	0.71	0.67	0.92	0.99	0.067	0.077	0.068	0.079	0.068	0.072	0.006
169	Tm	0.43	0.43	1.95	1.70	2.23	2.40	0.091	0.107	0.088	0.104	0.104	0.099	0.009
174	Yb	2.76	2.60	0.37	0.34	0.54	0.58	0.178	0.176	0.173	0.189	0.192	0.182	0.008
175	Lu	0.41	0.40	1.80	1.72	1.83	2.02	0.115	0.129	0.107	0.130	0.108	0.118	0.011

To evaluate the instrumental repeatability of the measured values and accuracy of data, analyses of geological standard reference materials (Govindaraju, 1994) from NIST (MAG, AGV and BHVO) were carried out according to the above mentioned procedures. The results obtained for the dissolution experiments carried out for each standard reference material are listed in Table VI.

All the solutions obtained after digestion procedures were directly analysed after a 1:50 dilution with 5% HNO_3 Merck ULTRAPUR® solution containing 100 ppt Rh as the internal standard.

The samples were treated under a laminar air flow clean bench to minimize contamination risks.

3 RESULTS

3.1 Dissolved REE Concentrations

The dissolved REE depth profiles (Fig. 2) show four main features: (1) a high variability of REE content in surface waters (0–35 m); (2) a decrease in REE concentrations in the 35–200 m deep water layer; (3) a regular increase in some REE concentrations down to about 300 m; (4) quasi-constant values down to the bottom of some stations.

Comparison of the vertical profiles for selected REEs (Fig. 2) among the studied stations suggests that generally, surface waters for each single station show 10–15% higher concentrations with respect to the intermediate layers. The high variability of concentration values measured among the different stations for the surface and intermediate waters is strongly reduced for the bottom waters, thus suggestive of a more homogeneous REE distribution in the deep part of the column water. Furthermore, contents of REE recorded in surface waters show the highest values for LREE, from La to Gd, than for HREE, from Tb to Lu, suggesting that the input of REE is strictly related to atmospheric origin.

Comparison of the central Mediterranean REE vertical profiles reported by Greaves *et al.* (1991) for two western Mediterranean stations (10707 and 10708) shows a high similarity for comparable depth intervals in terms of absolute values, and RSD except for surface waters, which are generally more enriched in the Strait of Sicily. Moreover, the REE concentrations measured at intermediate depths are very similar to those reported by Bau *et al.* (1997) for oxic Levantine Intermediate Waters in the South Kasos basin (eastern Mediterranean), although HREE concentrations in the eastern basin are slightly higher in relation to the occurrence of HREE enriched rocks outcropping in many regions on the eastern basin (Koepke *et al.*, 2002).

3.2 Particulate REE Concentrations

To show the REE behaviour in vertical profiles of particulate REE contents, the S128, S24 and S455 stations were selected to provide information from different sampling areas: S128 for the Gulf of Gela, S24 for the Ionian Sea and S455 for the Strait of Sicily far from the coastline. The REE distribution along these log profiles (Fig. 3) shows increasing REE contents in suspended particulate with depth at the S-128 station. In the station S-455 station, this effect is evident for La, Ce and Nd but is not observed at S24 site at all.

The shale normalized REE values calculated vs. PAAS (Taylor and McLennan, 1985) and the related patterns for surface (0–35 m), intermediate (35–100 m) and deep (>300 m) suspended particulate matter are reported in Figure 4:

- a regular behaviour with slight enrichment of LREE vs. HREE in surface waters both in samples closer to the coastline (stations S128 and S24) and in samples from the Strait of Sicily (S-455);

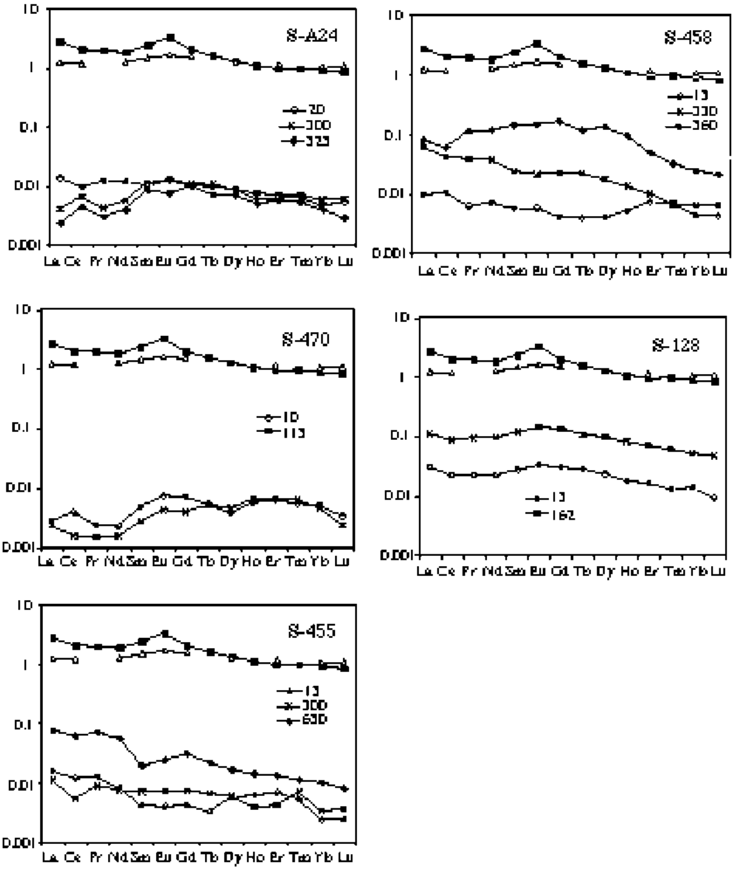

FIGURE 4 Shale-normalized REE patterns in suspended particulate from surface, intermediate and deep seawater samples. The shale-normalized REE patterns of volcanic ashes (■) and Saharan dust (△) from Greaves *et al.* (1994) are shown for comparison. Numbers in the legends denote the sampling depths.

- a high degree of LREE/HREE fractionation in suspended particulate from intermediate and deep water samples in the Strait of Sicily (S455);
- a flat behaviour with enrichment in intermediate REE contents.

The reported shale-normalized REE patterns of the particulate matter analysed from the 0–35 m water layer show positive Eu anomalies ($\mathrm{Eu}/\mathrm{Eu}^* > 1$) that generally mirror the same parameter measured form surface waters at the same stations (Tabs. I and II).

4 DISCUSSION

4.1 Dissolved REE Concentrations

Comparison between dissolved REE concentrations, salinity and temperature profiles measured for the same stations suggests that the 3-D circulation system of the basin directly drives the trace-element vertical distribution in the studied area.

In particular, the threefold stratification for the REE depth profiles recorded at the 10 stations reflects the typical three layers structure of the central Mediterranean area described by Morley *et al.* (1997): surface waters (0–35 m), Modified Atlantic Waters

(MAW, 35–200/250 m) and Levantine Intermediate Waters (LIW, 200/250–500/700 m). In particular, salinity profiles for the different stations record the classic sub-surface decrease related to the MAW eastward water flux and the sharp increase related to the westward LIW flowing (e.g., Robinson *et al.*, 1999). The occurrence of the above-mentioned three layers structure in the studied area justifies the similarities occurring between surface and intermediate waters sampled in this study and the good similarity with data reported by Greaves *et al.* (1991) for two western Mediterranean stations and by Bau *et al.* (1997) for REE concentrations of intermediate waters from the Levantine Mediterranean area.

Shale-normalized REE patterns (Fig. 5) of surface water REE data are higher than those of the adjacent north-east Atlantic (Greaves *et al.*, 1991) but show a similar pattern. This suggests a common origin for the two groups of seawater samples and an important contribution of Mediterranean inputs characterized by large riverine and aoelic inputs of silicatic crustal materials.

4.2 Atmospheric Aerosol

Mineralogical assemblages occurring in the "Red dust" and ashes from the Etna volcano are reported in Figure 6. The mineralogical composition of "Red dust" is dominated by a quartz-kaolinite assemblage, in good agreement with data from Molinaroli (1996), while ashes from Etna volcano consist of a characteristic magmatic paragenesis with Ca-rich plagioclase and clinopyroxene. The REE distribution and shale-normalized ratios measured in "Red dust" and ashes from the Etna volcano are reported in Table VII.

Positive Eu anomalies were measured in the bulk fraction of the Etna volcano (average of 1.51) while Saharan dust showed an Eu* of about 1.0–1.1. The high anomalies measured in the Etna volcanic ashes can be explained by the abundance of plagioclase minerals (Fig. 6). However, the mineralogical composition of Saharan red dust essentially consists of residual phases (Molinaroli, 1996; Tomadin *et al.*, 1996) as quartz and phyllosilicates (and poor plagioclase), thus explaining the different Eu anomaly in these materials.

4.3 Origin of the Surface Particulate Distribution

In the petrologic systems, the LREE/HREE fractionation is strictly related to the occurrence of partial fusion phenomena during which the less compatible LREEs are preferentially enriched in liquids with respect to the more compatible HREE. Conversely, the anthropogenic input of REE is very distinctive, especially if related to the occurrence of oil-refineries because LREE are strongly enriched in petroleum-cracking catalysts, thus producing very high $(La/Yb)_n$ ratios. Moreover, the input of REE in the oceans being mainly due to continental runoff (Tachikawa *et al.*, 1999a), the degree of Eu anomaly in suspended particulate is essentially driven by the original composition of continental input. Also, Eu/Eu* values are essentially related to preferential removal of Eu under magmatic conditions because, during weathering, Eu is not fractionated with respect to other REE. Moreover only materials of magmatic origin can show $Eu/Eu^* \neq 1$ values while both anthropogenic and authigenic fractions of suspended particulate are formed during processes unaffected by Eu fractionations. Therefore, $(La/Yb)_n - Eu/Eu^*$ space diagrams are suitable for distinguishing between, anthropogenic and lithogenic imprints on seawater particulate matter.

In the $(La/Yb)_n - Eu/Eu^*$ space diagram (Fig. 7), our surface particulate samples fall in the area delimited by three different hyperbolas obtained under the hypothesis of mixing among three different End Members: (1) a "lithogenic fraction" related to the volcanic rocks from the Etna volcano (EM 1), (2) an "anthropogenic signature" (EM 2) and (3) an "autigenic" particulate fraction (EM 3).

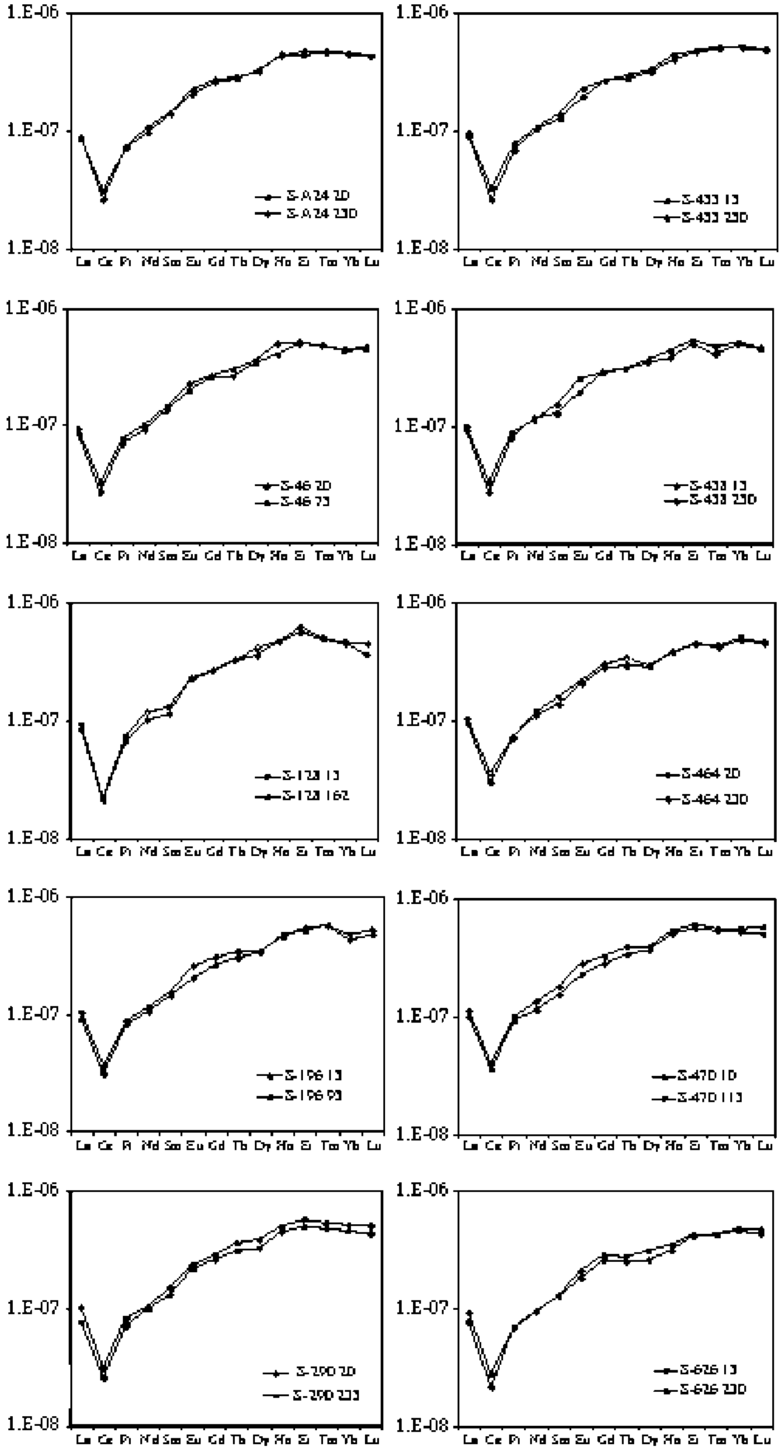

FIGURE 5 Shale-normalized REE patterns in surface and intermediate seawater samples. Numbers in the legends denote the sampling depths.

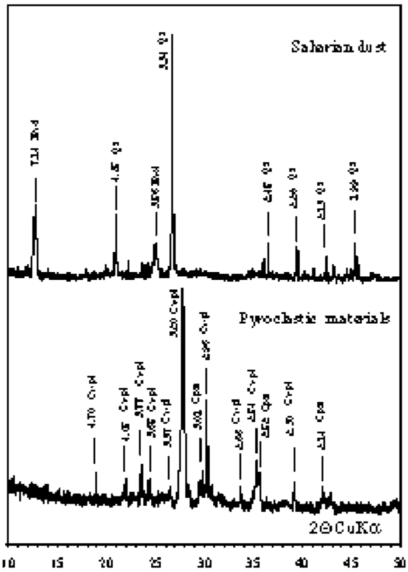

FIGURE 6 X-ray diffraction patterns for Saharan dust and pyroclastic materials from Etna volcano. Qz: quartz; Kaol: kaolinite; Cpx: clinopyroxene; Ca-pl: Ca-rich plagioclase.

The values representative of the "Lithogenic" end member EM 1 are obtained from rock samples of alkaline suite lavas of the Etna volcano (Cristofolini *et al.*, 1981).

The values reported for the anthropogenic inputs EM 2 highlight the distinctive REE signature of minerals as bastnaesite (Ce,La)CO_3F and monazite (Ce,La)PO_4 (Olmez *et al.*, 1990), extensively used as cracking catalysts in the oil-refining industries (Neary and Highley, 1989). Because of the "lanthanide contraction", these minerals (especially the bastnaesite) are strongly enriched in LREE with very high $(La/Yb)_n$ ratios, thus indicating their occurrence in the suspended particulate mixture.

TABLE VII REE concentrations (ppm) measured in pyroclastic products from M. Etna.

	Etna	*Sahara*
La	106.09	46.80
Ce	162.05	92.80
Pr	17.27	
Nd	61.56	42.70
Sm	13.07	8.11
Eu	3.58	1.77
Gd	9.47	7.00
Tb	1.22	
Dy	6.09	5.86
Ho	1.08	
Er	2.75	3.25
Tm	0.39	
Yb	2.57	2.97
Lu	0.36	0.46
[La/Yb]N	3.04	1.16
Eu/Eu*	1.51	1.11

Note: Analogous concentrations reported for Saharan dust are from Greaves *et al.* (1994).

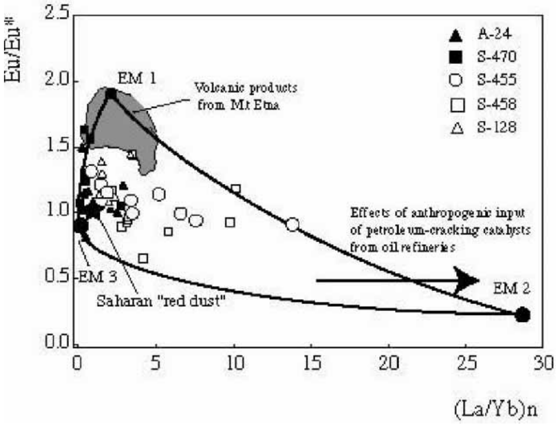

FIGURE 7 $(La/Yb)_n$ vs. Eu/Eu* space diagram with reported samples of suspended particulate. ◆: samples from S455 station. ▲: samples from deep water masses. □: samples from intermediate water masses. ○: samples from surface waters. ●: authigenic particulate matter from Sargasso Sea and Indian Ocean reported as reference.

Conversely, the shale-normalized REE distribution of authigenic particulate fraction is usually driven by oxidative precipitation of Mn as MnO_2 and removal of REE (III) by absorption on particulate MnO_2 surface and oxidation of Ce (III) to CeO_2 at shallow depths (Sholkovitz *et al.*, 1994; Alibo and Nozaki, 1999). A preferential uptake of LREE relative to HREE is strictly related to this process by desorption at deeper depths. This phenomenon in the surface water masses of the Sargasso Sea yields a $(La/Yb)_n$ close to 0.23 and an Eu/Eu* ratio close to 0.9 (Bertram and Elderfield, 1993). As the fractionation between seawater and suspended authigenic particulate is similar in the Sargasso Sea, Indian Ocean (De Baar *et al.*, 1985) and tropical Atlantic Ocean (De Baar *et al.*, 1983), we assumed these values to be representative of the authigenic particulate fraction in seawater.

In the $(La/Yb)_n - Eu/Eu^*$ space diagram, the samples of particulate collected from shallow and intermediate waters (at depths of 0–35 m and 35–200 m, respectively) fall between the Etna and Saharan dust ranges values, while deep particulate samples (only for the stations S24, S128 and S455) fall along the hyperbolic array of $[La/Yb]_N$ values greater than 4 and Eu/Eu* values close to 1 typical of the EM2. Therefore, in shallow and intermediate water masses, the contribution of the lithogenic fraction to the suspended particulate is at a maximum, while in deep waters, the presence of waste materials dominates. The origin of these anthropogenic signatures could be located in the Gulf of Gela where a large chemical and oil-refined petroleum industry is present. This hypothesis is confirmed by the behaviour of Eu/Eu* and $[La/Yb]_N$ values in the S128 and S455 stations, near the Gulf of Gela, where the suspended matter fits very well with the hyperbolic array.

5 CONCLUSIONS

The recorded distribution of seawater REE in the Sicily Channel seawaters follows the well-known threefold stratification recorded using classic S-T hydrographic parameters with a shallow water layer, an intermediate water mass represented by the eastward current of the Modified Atlantic Waters and a deep westward water flux due to the outflow of the salty Levantine Intermediate Water. This provides the opportunity to integrate physical and chemical data to estimate variations of fluxes in time and space related to local and wide-scale oceanographic events.

Analysis of REE in suspended particulate highlights an important mixing effect among two main end-members:

- a lithogenic component consisting of a mixture of volcanic products, possibly of the Etna volcano and "Red dust" of Saharan origin;
- a component representative of anthropogenic inputs with a REE signatures markedly different from the others, and essentially due to oil-refining and chemical industries located in the part of the Strait of Sicily close to the Gulf of Gela.

Further research is being planned to estimate the effects of chemical interactions between suspended particulate and seawater in the studied area which could contribute to a better understanding of the "trace-element concentration effect", making the Mediterranean region an important source area for the chemistry of the open ocean.

Acknowledgements

We thank Dr Riccardo Melfa for his help during sample collection and handling. We thank the staff of the RV *Urania.* This research was supported by the European project N. MED/96–052, "Distribution, Biology and Biomass Estimates of the Sicilian Channel Anchovy" and by "Progetto Attività Oceanografiche of CNR". We are also indebted to Massimo Burzio of the Italian C.N.R.

References

Alibo, D. S. and Nozaki, Y. (1999). Rare earth elements in seawater: Particle association, shale-normalization, and Ce oxidation. *Geochimica et Cosmochimica Acta*, **63**, 363–372.

Barbante, C., Cozzi, G., Capodaglio, G., Van de Velde, K., Ferrari, C., Boutron, C. and Cescon, P. (1999). Trace element determination in alpine snow and ice by double focusing inductively coupled plasma mass spectrometry with microcentric nebulization. *Journal of Analytical and Atomic Spectroscopy*, **14**, 1433–1438.

Bau, M., Moller, P. and Dulski, P. (1997). Yttrium and lanthanides in eastern Mediterranean seawater and their fractionation during redox cycling. *Marine Chemistry*, **56**, 123–131.

Bertram, C. J. and Elderfield, H. (1993). The geochemical balance of rare earth elements and neodymium isotopes in the oceans. *Geochimica et Cosmochimica Acta*, **57**, 1957–1986.

Cristofolini, R., Albini, A., Di Girolamo, P. and Stanzione, D. (1981). Geochemistry of some volcanic rocks from south-eastern Sicily: Rare Earth and other trace elements distribution. *Bulletin of Volcanology*, **44**, 95–107.

De Baar, H. J. W., Bacon, M. and Brewer, P. G. (1983). Rare-earth distributions with positive Ce anomaly in the western North Atlantic Ocean. *Nature*, **301**, 324–327.

De Baar, H. J. W., Brewer, P. G. and Bacon, M. D. (1985). Anomalies in rare-earth distributions in seawater: Gd and Tb. *Geochimica et Cosmochimica Acta*, **49**, 1961–1969.

Elbaz-Poulichet, F., Guieu, C. and Morley, N. H. (2001). A reassessment of trace metal budgets in the Western Mediterranean Sea. *Marine Pollution Bulletin*, **42**, 623–627.

Elderfield, H. and Greaves, M. J. (1982). The rare earth elements in seawater. *Nature*, **296**, 214–219.

FengFu, F., Shinotsuka, K., Ebihara, M. and Akagi, T. (1997). Distribution ratio of dissolved and particulate REE in surface coastal seawater. *Geochemical Journal*, **31**, 303–314.

Frost, C. D., O'Nions, R. K. and Goldstein, S. L. (1986). Mass balance for Nd in the Mediterranean Sea. *Chemical Geology*, **55**, 45–50.

Goldstein, S. L., O'Nions, R. K. and Hamilton, P. J. (1984). An Sm–Nd isotopic study of atmospheric dusts and particulates from major river systems. *Earth and Planetary Science Letters*, **70**, 221–236.

Govindaraju, K. (1994). Compilation of working values and sample descriptions for 383 geostandards. *Geostandard Newsletter*, Special Issue, **18**, 1–158.

Greaves, M. J., Elderfield, H. and Sholkovitz, E. R. (1994). Aeolian sources of rare earth elements to the Western Pacific Ocean. *Marine Chemistry*, **68**, 31–37.

Greaves, M. J., Rudnicki, M. and Elderfield, H. (1991). Rare earth elements in the Mediterranean Sea and mixing in the Mediterranean outflow. *Earth and Planetary Science Letters*, **103**, 169–181.

Grousset, F. E., Henry, F., Minster, J. F. and Monaco, A. (1990). Nd isotopes as tracers in water column particles: the western Mediterranean Sea. *Marine Chemistry*, **30**, 389–407.

Güllü, G. H., Olmez, I. and Tuncel, G. (2000). Temporal variability of atmospheric trace element concentrations over the eastern Mediterranean Sea. *Spectrochimica Acta*, **B55**, 1135–1150.

Hanson, G. N. (1989). An approach to trace element modelling using a simple igneous system as an example. In: Lipin, B. R. and McKay, G. A. (eds.), *Geochemistry and Mineralogy of Rare Earth Elements. Reviews in Mineralogy*. Mineralogical Society of America, Washington D.C., Vol. 21, pp. 79–98.

Koepke, J., Seidel, E., and Kreuzer, H. (2002). Ophiolites on the Southern Aegean islands Crete, Karpathos and Rhodes: composition, geochronology and position within the ophiolite belts of the Eastern Mediterranean. *Lithos*, **65**, 183–203.

McKay, G. A. (1989). Partitioning of rare earth elements between major silicate minerals and basaltic melts. In: Lipin, B. R. and McKay, G. A. (eds.), *Geochemistry and Mineralogy of Rare Earth Elements. Reviews in Mineralogy*. Mineralogical Society of America, Washington D.C., Vol. 21, pp. 45–75.

Molinaroli, E. (1996). Mineralogical characterisation of Saharan dust with a view to its final destination in Mediterranean sediments. In: Guerzoni, S. and Chester, R. (eds.), *The Impact of Desert Dust Across the Mediterranean*. Kluwer Academic, Dordrecht, Netherlands, pp. 153–162.

Möller, P., Dulski, P. and Luck, J. (1992). Determination of rare earth elements in seawater by inductively coupled plasma-mass spectrometry. *Spectrochimica Acta*, **47B**, 1379–1387.

Morley, N. H., Burton, J. D., Tankere, S. P. C. and Martin, J. M. (1997). Distribution and behaviour of some dissolved trace metals in the western Mediterranean Sea. *Deep Sea Research*, **44**, 675–691.

Neary, C. R. and Highley, R. J. (1989). The economic importance of the rare earth elements. In: Henderson, P. (ed.), *Rare Earth Elements Geochemistry*, 3rd ed. Elsevier, Amsterdam.

Olmez, I., Sholkovitz, E. R., Herman, D. and Eganhouse, R. P. (1990). Rare earth elements in sediments off Southern California. *Environmental Science and Technology*, **25**, 310–316.

Paulson, A. J. (1986). The effects of flow rate and pre-treatment on the analyses of trace metals in estuarine and coastal seawater by Chelex-100. *Analytical Chemistry*, **58**, 183–187.

Robinson, A. R., Sellschopp, J., Warn-Varnas, A., Leslie, W. G., Lozano, C. J., Haley, P. J., Jr., Anderson, L. A. and Lermusiaux, P. F. J. (1999). The Atlantic Ionian stream. *Journal of Marine Systems*, **20**, 129–156.

Sholkovitz, E. R., Landing, W. M. and Lewis, B. L. (1994). Ocean particle chemistry: The fractionation of rare earth elements between suspended particles and seawater. *Geochimica et Cosmochimica Acta*, **58**, 1567–1579.

Tachikawa, K., Jeandel, C. and Roy-Barman, M. (1999a). A new approach to the Nd residence time in the ocean: the role of atmospheric inputs. *Earth and Planetary Science Letters*, **170**, 433–446.

Tachikawa, K., Jeandel, C., Vangriesheim, A. and Dupré, B. (1999b). Distribution of rare earth elements and neodymium isotopes in suspended particles of the tropical Atlantic Ocean (EUMELI site). *Deep Sea Research*, **46**, 733–755.

Taylor, S. R. and McLennan, S. M. (1985). *The Continental Crust: Its Composition and Evolution*. Blackwell Scientific, Oxford.

Tomadin, L., Wagenbach, D. and Landuzzi, V. (1996). Mineralogy and source of high altitude glacial deposits in the western Alps: Clay minerals as Saharan dust traces. In: Guerzoni, S. and Chester, R. (eds.), *The Impact of Desert Dust Across the Mediterranean*. Kluwer Academic, Dordrecht, Netherlands, pp. 223–232.